ESRF	**Experiment title:** Statistical study of the mechanical deformation of nanocrystals	**Experiment number**: MA-3056
Beamline: ID01	**Date of experiment**: from: 30/09/2016 to: 05/10/2016	**Date of report**: 14/03/2017
Shifts: 15	**Local contact(s)**: Steven Leake	*Received at ESRF:*

Names and affiliations of applicants (* indicates experimentalists):

Beutier Guillaume* (SIMaP)
Comby Solène* (SIMaP)
Verdier Marc* (SIMaP)
Volpi Fabien* (SIMaP)

REPORT

The purpose of the experiment was to perform a statistical study of the microstructure of gold nanocrystals before and after nanoindentation. We used the high throughput of ID01 for Coherent X-ray Diffraction (CXD) measurements and of the nanoindentation facility of our lab, also based in Grenoble, to measure a large number of crystals by CXD *before* and *after ex situ* nanoindentation, during the same experimental run.

The experiment went almost as initially planned and was very successful.

The gold nanocrystals were prepared by solid state dewetting of a gold thin film on a sapphire substrate. The substrates were covered with a patterned mask in order to obtain well isolated crystals aligned on a square lattice (Figure 1). The large separation is needed for the CXD measurements because the focused beam has weak but large tails that can cause the measurement to fail by illuminating nearby crystals. The template is used to identify the crystals individually during the nanoindentation and the CXD measurements. SEM prior to the experiment allowed do identified the best crystals, i.e. the ones that display a shape as close as possible to the Winterbottom equilibrium shape. This characteristic is important to ease the modelling, and allows to select a set of crystals with external shapes as similar as possible, in order to make statistics.

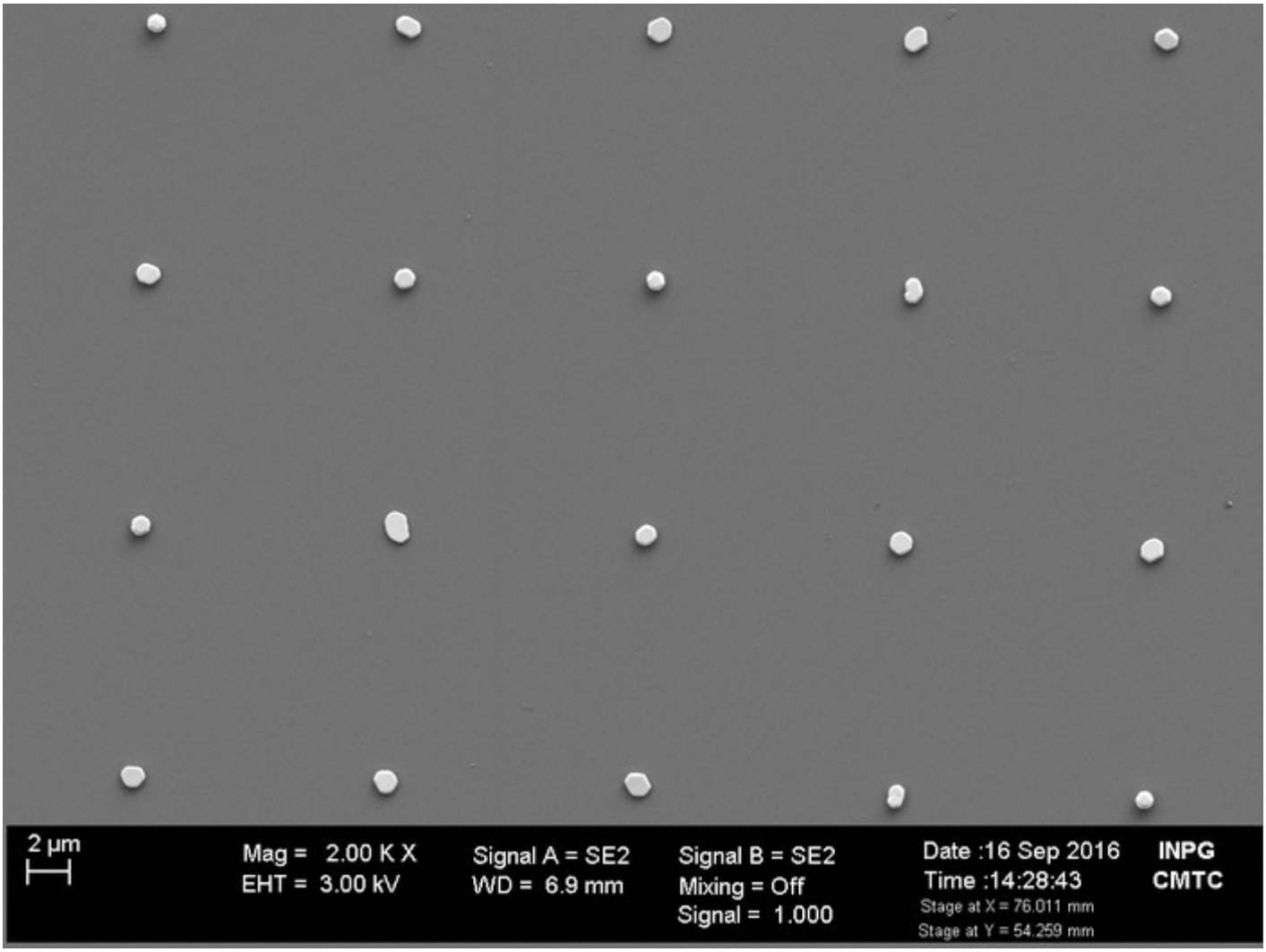

Figure 1: typical SEM view of the nanocrystals.

We prepared 2 substrates hosting slightly different types of crystals: they were obtained by dewetting films of different thickness (45 nm and 60 nm), leading to nanocrystals with slightly different average sizes. The influence of the size on the mechanical behaviour is an open debate in the community.

As initially planned, a large number of crystals on both substrates were sequentially measured in their initial state, then indented in our lab, then measured again at ID01. The full list of crystals is given in appendix. The beamtime was fully used, by measuring one of the samples while indenting the other one. In addition, due to the larger through-put of CXD than nano-indentation, a large number of crystals were measured only by CXD, for future investigation of their mechanical response: the initial microstructure is relevant to understand it. Characterisation of the final microstructure, if needed, can be done later (beamtime will be required).

Different parameters of indentation were used. Some crystals were loaded with a “flat punch” and others were properly indented with a “cube corner” tip (Figure 2). In all cases, the load-displacement curves, which characterize globally the mechanical test, were recorded, and the crystals were loaded/indented at various load levels and depths.

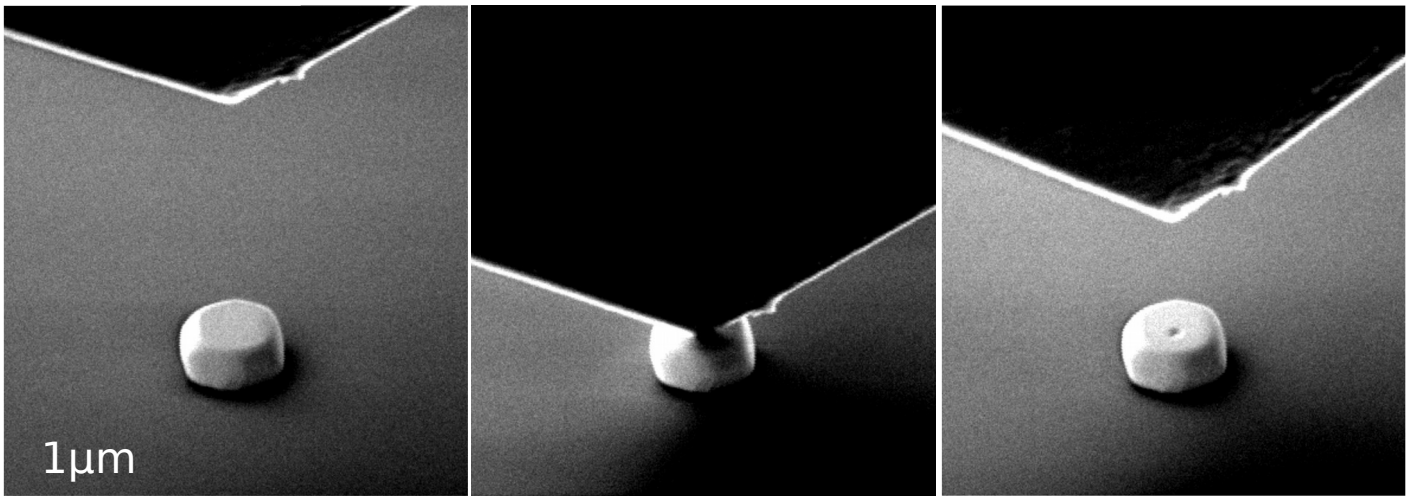

Figure 2: Example of nanoindentation with a cube corner tip.

The CXD experiment was performed with the standard set-up, i.e. at 8 keV with Fresnel Zone Plate focusing (the sample was placed 1 mm out of focus in order to match the beam size with the crystals size). The vicinity of the 111 Bragg reflection was measured in 3D by rocking the sample and recording the diffraction pattern with the Maxipix4 detector. Sufficient oversampling in the 3 dimensions was ensured by the detector to sample distance (~1m) and the rocking curve step size (0.005°).

We intend to recover real space images of the crystals by using phase retrieval algorithms. The phase of the real space reconstruction provides an image of lattice displacement field, from which the strain and the crystal defects can de deduced. The analysis is in progress, but will take time due to the large amount of data and the poor automation of the "reconstruction" process. In cases when the real space reconstruction fails, a reciprocal space analysis can already provide qualitative information on the microstructure of the crystal, before and after indentation.

We provide below an example of data with its real space reconstruction, for a crystal which has been loaded by a flat punch. The force-displacement curve suggests a reversible (elastic) load (Figure 3), but the diffraction data proves that the load induced stacking faults in the {111} planes (Figure 4) that were not detected by the nanoindenter. This example demonstrates the high sensitivity of CXD to crystal defects, to a level that even top-of-the-art mechanical apparatus cannot challenge.

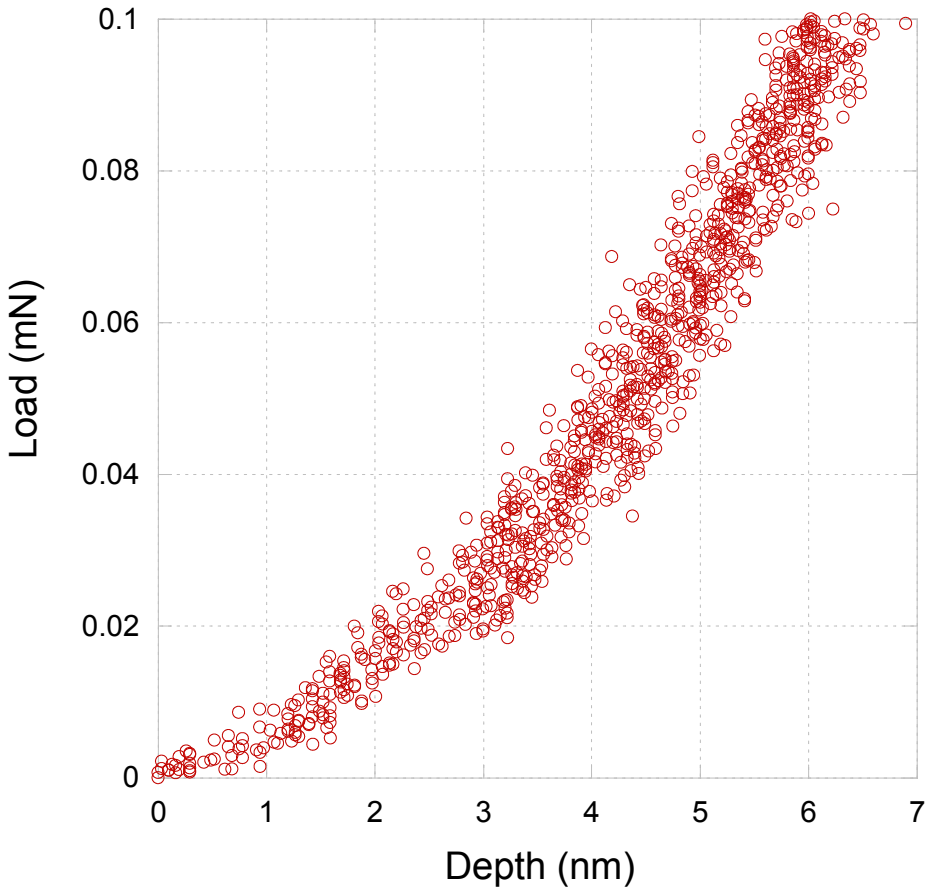

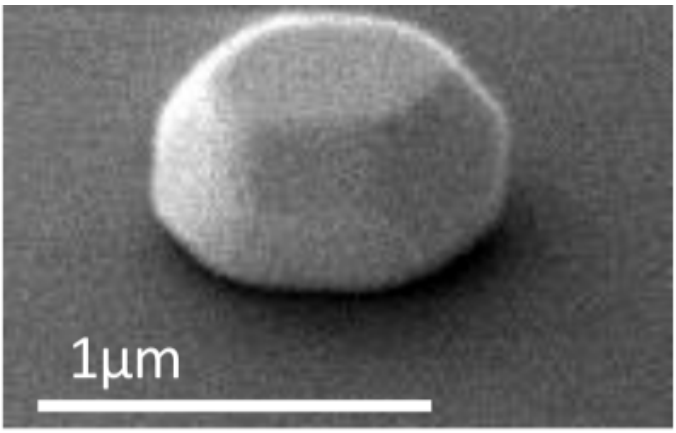

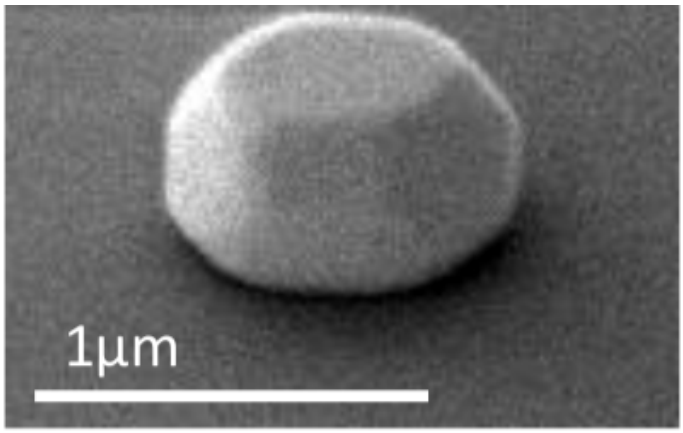

Figure 3: Reversible indentation of gold nanocrystal with a flat punch. The load-depth curve does not display any discontinuity (a sign of dislocation avalanches) and suggests a reversible mechanical behaviour. The SEM images of the crystal before (left) and after (right) indentation are identical.

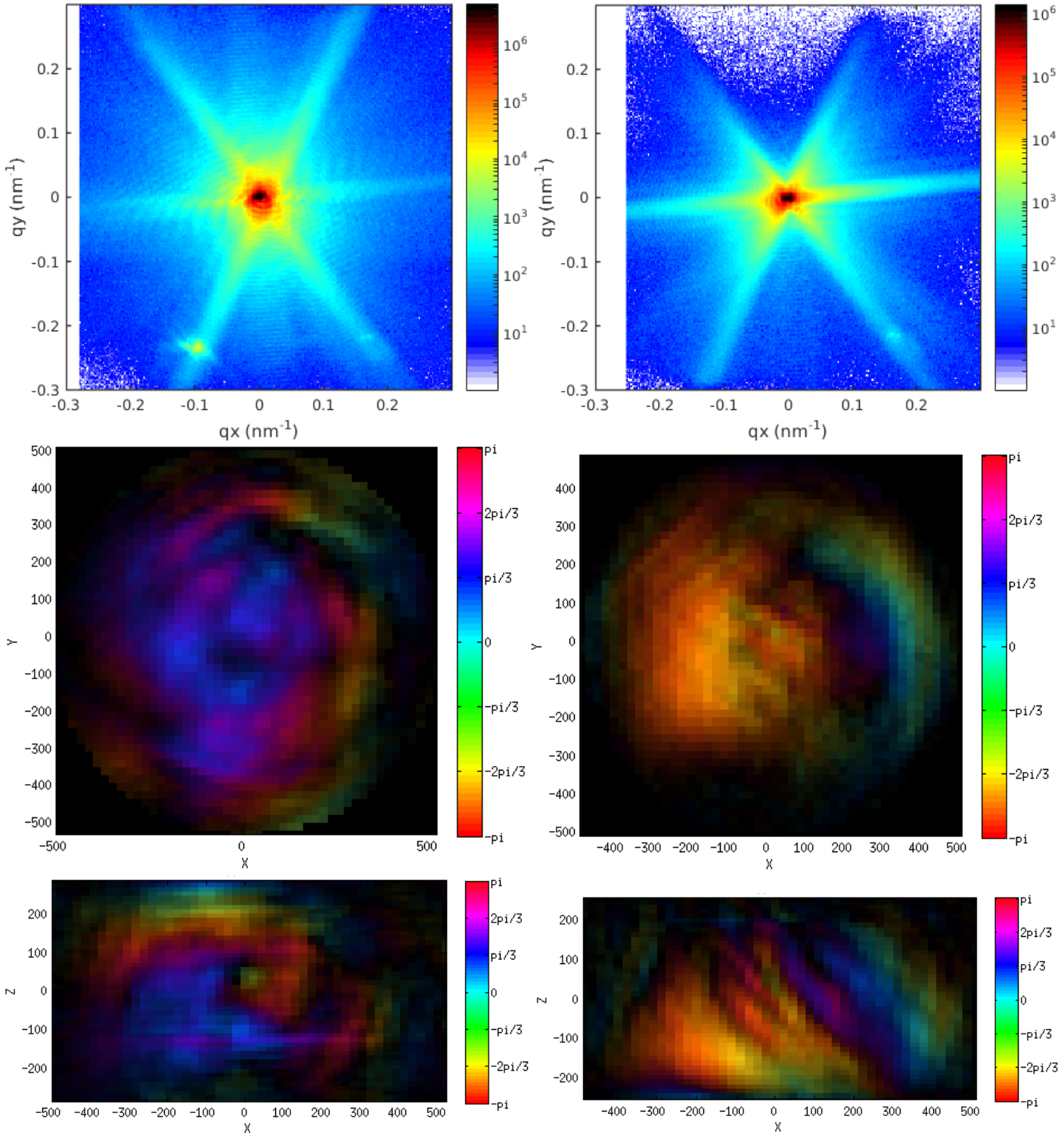

Figure 4: Projection of the CXD patterns along the 111 growth axis, before and after flat-punch loading, and the corresponding real-space reconstructions (x-y cuts and x-z cuts). The scale in the real space images is in nm. The colour encodes the phase, whose jumps reveal the presence of crystal defects. The phase origin is irrelevant.

While the analysis is still in progress, we can already draw the following general conclusions:

- We established a reliable procedure to investigate the effect of mechanical loading on the microstructure of nanocrystals.
- The method is high throughput, because both techniques (CDI and nanoindentation) are high throughput and both located in Grenoble.

- The large number of crystals measured in this run will provide interesting mechanical information, but probably deserve more measurements in order to improve the statistical validity of study.

APPENDIX

Full list of the nanocrystals measured by CXD during this experiment, with their corresponding mechanical tests.

		CRYSTAL SIZE (SEM&AFM)			Nano-indentation					CXD scans	
							first pop-in				
SAMPLE	CRYSTAL	Lx (nm)	Ly (nm)	Lz (nm)	Indenter	Maximal force (mN)	Force at (mN)	Length of (nm)	Displacement before (nm)	scan before (file “45nm”)	scan after (file “45nm_2”)
SAMPLE “45 nm”	1,3	702	669	520	Flat Punch	0.4			reversible	23	75
	1,4	753	758	330	Cube Corner	0.06			reversible	29	78
	1,5	744	697	364	Cube Corner	0.03			reversible	31	80
	1,6	711	720							44	
	1,7			460						46	
	2,3				Flat Punch	0.91	0.91	300.05	31.46	18	72
	2,4	669	651	620						37 & 38	83
	2,7			316						48	
	3,2	353	367	205	Flat Punch	0.1			reversible	18	97
	3,6									53	
	3,8									55	
	4,3	739	748	414	Cube Corner	0.0091	0.0091	4	5.6	25	89
	4,4	758	748	266						27	
	4,7			330						57	
	5,2	763	790	348	Cube Corner	0.0093	0.0093	8.6	5	20	87
										21	
	5,4	758	734	330	Cube Corner	0.0078	0.0078	6.52	4.33	35	85
	5,6									59	
	6,5	790	781	270	Cube Corner	0.0157	0.0157	17.21	6.92	33	92
	6,6									62	
	6,8									65	
	7,4	702	702	385						40 & 41	94
	7,7			263						67	
	8,4	697	683	390						69	
	8,8									71	
	9,7			248						78	
	10,2	744	720	400						82	
	10,4	749	739	365						80	
	10,6									84	
	11,5	762	725							73	
	12,6									75	
	13,2	772	776	353						90	

		CRYSTAL SIZE (SEM&AFM)			Nano-indentation					CXD scans	
							first pop-in				
SAMPLE	CRYSTAL	Lx (nm)	Ly (nm)	Lz (nm)	Indenter	Maximal force (mN)	Force at (mN)	Length of (nm)	Displacement before (nm)	scan before (file “60nm”)	scan after (file “60nm_2”)
SAMPLE “60 nm”	7,2	1070	1100	320						26	54
	8,2	880	950	527	Flat Punch	0.1			reversible	29	23
	2,3	900	940	603						38	
	7,3	970	970	416	Cube Corner	0.005	0.005	1.89	3.07	35	29
	8,3	860	1040	450	Cube Corner					33	
	10,3	860	865	550	Cube Corner	0.0056	0.0056	3.95	3.259	31	26
	11,3	860	860	590							89
	7,4	950	1060	390						43	62
	10,4	1049	1065	330	Cube Corner	0.0074	0.0074	4.868	4.113	46	32
	3,5	1170	1150	267	Flat Punch	0.46	0.46	73.46	11.19	53	
	4,5	1050	1000	355	Flat Punch	0.04	0.04	1.35	9.8		52
	7,5	1000	820	480	Cube Corner	0.0094	0.0094	8.73	4.88	51	38
	10,5	1210	1300	230	Cube Corner	0.006	0.006	1.5	5.3	49	35
	4,6	950	1090							55	57
	5,6	1000	850	478	Cube Corner	0.008	0.008	2.65	6.65	57	42
	8,6	820	975	490	Cube Corner	0.008	0.008	5.49	5.24	60	
	1,7	1070	1160	281						73	
	4,7	850	840	588						68	
	5,7	1040	1170	315						65	75
	6,7	860	795	593						63	
	5,8	960	1000	431						75	
	11,8	990	1300	265							92
	4,9	920	820	485						77	
	6,10	813	930	612							85
	8,10	980	880	420	Cube Corner	0.014			reversible	79	46
	10,10	1020	930	435							81
	1,11	1200	820	350							77
	3,11										87
	7,11	990	1000	607						81	99+
	5,12										69
	2,13	1140	1160	346							60
	6,13	1040	1030	360							64